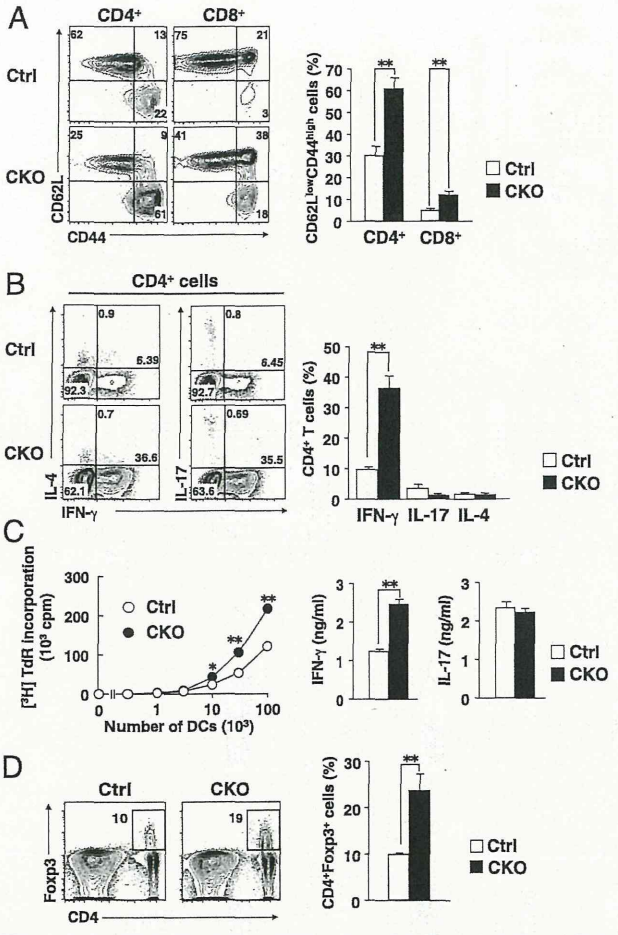

FIGURE 5. High frequency of Th1 cells and increased ability of DCs to promote differentiation of $CD4^+$ T cells into Th1 cells in Shp1 CKO mice. (**A**) Splenocytes from control or Shp1 CKO mice at 20–24 wk of age were stained for CD62L, CD8, CD44, and CD4 as well as with PI, and the expression of CD44 and CD62L on viable $CD4^+$ or $CD8^+$ cells was analyzed by flow cytometry. The percentage of activated ($CD62L^{low}$ $CD44^{high}$) $CD4^+$ or $CD8^+$ cells among all viable $CD4^+$ or $CD8^+$ cells was determined; data are means ± SE for a total of five mice per group examined in three independent experiments. $^{**}p < 0.01$ (Student *t* test). (**B**) Splenocytes from control or Shp1 CKO mice at 20–24 wk of age were stimulated with PMA (100 ng/ml) and ionomycin (1 μg/ml) for 4 h in the presence of GolgiPlug. The cells were then stained for CD4, fixed, permeabilized, and stained again for IFN-γ and either IL-4 or IL-17A. The intracellular expression of IFN-γ, IL-17, or IL-4 in $CD4^+$ cells was then analyzed by flow cytometry. The percentage of cells that express IFN-γ, IL-17, or IL-4 among total $CD4^+$ cells was determined; data are means ± SE for a total of five mice per group examined in three independent experiments. $^{**}p < 0.01$ (Student *t* test). (**C**) Control or Shp1 CKO mice at 12–16 wk of age were injected intravenously with 3 mg OVA. After 12 h, splenic $CD11c^+$ DCs were isolated from the mice and were cultured for 72 h at various densities with $CD4^+$ T cells (1×10^5) from OT-II mice. Cell proliferation (*left panel*) as well as the concentrations of IFN-γ and IL-17 in culture supernatants (*right panels*) were then determined. Data are means ± SE of triplicate determinations and are representative of three separate experiments. $^{*}p < 0.05$, $^{**}p < 0.01$ (versus the corresponding value for control mice or for the indicated comparison; Student *t* test). (**D**) Splenocytes from control or Shp1 CKO mice at 20–24 wk of age were stained for CD4, fixed, permeabilized, and stained again for Foxp3. The intracellular expression of Foxp3 in $CD4^+$ cells was then analyzed by flow cytometry. The percentage of $CD4^+Foxp3^+$ cells among total $CD4^+$ splenocytes was determined; data are means ± SE for a total of five mice per group examined in three independent experiments. $^{**}p < 0.01$ (Student *t* test).

in the thymus (44). The frequency of either single-positive (CD4 or CD8), double-positive, or double-negative (DN1 to DN4) thymocytes, however, did not differ between Shp1 CKO and control mice (Supplemental Fig. 3).

Increased number of B-1a cells and elevation of serum concentrations of IgM and IgG2a in Shp1 CKO mice

Given that the frequency of B cells in the spleen of Shp1 CKO mice was about twice that for control mice (Fig. 2C), we examined the effect of DC-specific Shp1 deficiency on B cell subpopulations in the spleen. The frequency of marginal-zone B cells ($CD21^{high}$ $CD23^{low}$) (45) among matured B cells ($B220^+AA4.1^-$) (45) was decreased in the spleen of Shp1 CKO mice at 10–12 wk of age compared with that for control mice (Fig. 6A), whereas the frequency of follicular B cells ($CD21^{high}CD23^{high}$) (45) did not differ between the two strains. The frequency of either T1 ($CD21^{high}$ $CD23^{high}$) or T2 ($CD21^{low}CD23^{low}$) B cells among immature B cells ($B220^+AA4.1^+$) did not differ between the two genotypes (Fig. 6A). The population of activated B cells ($B220^+CD69^+$) (46) among $B220^+$ B cells was markedly increased compared with that for control mice at 10–12 wk of age (Fig. 6B), suggesting that Shp1 deficiency in DCs results in activation of B cells in the spleen.

Mature splenic B cells consist mostly of two subtypes, B-1a and B-2 cells (47). B-1a cells constitute a relatively small subpopulation of splenic B cells defined by the expression of CD5, and they spontaneously secrete IgM. The number of B-1a cells is markedly increased in the spleen of *motheaten* mice (20). The proportion of $CD19^+CD5^+$ (B-1a) cells among splenocytes of Shp1 CKO mice was markedly increased compared with that for control mice at 10–12 wk of age (Fig. 6C), suggesting that Shp1 deficiency in DCs affects development of B-1a cells in the spleen. To examine further the effect of DC-specific Shp1 deficiency on B cell function, we measured the concentrations of Ig isotypes in serum. The serum concentrations of IgM and IgG2a were markedly increased in Shp1 CKO mice at 20–24 wk of age compared with those apparent for control mice, whereas the levels of IgA, IgG1, IgG2b, and IgG3 did not differ between the two strains (Fig. 6D).

DCs are an important source of BAFF and APRIL, both of which are thought to promote B cell survival and plasmablast differentiation (48). However, the amounts of BAFF and APRIL mRNAs in splenic $CD11c^+$ DCs did not differ between control and Shp1 CKO mice (Supplemental Fig. 4).

Shp1 CKO mice develop autoimmunity

Motheaten mice develop systemic autoimmune disease such as glomerulonephritis and interstitial pneumonitis, with accompanying hypergammaglobulinemia, high titers of autoantibodies, and immune complex deposition (20) We therefore next investigated whether Shp1 CKO mice similarly develop autoimmune disease. H&E staining revealed massive leukocyte accumulation and hypercellularity in renal glomeruli as well as prominent leukocyte infiltration at lung alveoli of Shp1 CKO mice at 36–40 wk of age (Fig. 7A–C), suggesting that aged Shp1 CKO mice develop glomerulonephritis as well as interstitial pneumonitis. In addition, the CKO mice at 20–24 wk of age manifested a slightly increased level of leukocyte accumulation at lung alveoli (data not shown). We also found that staining for IgG and C3, which reflects immune complex deposition, was markedly increased in renal glomeruli of aged Shp1 CKO mice (Fig. 7D, 7E). Consistent with the histological data, aged Shp1 CKO mice manifested impairment of the renal function, as the levels of blood urea nitrogen and of

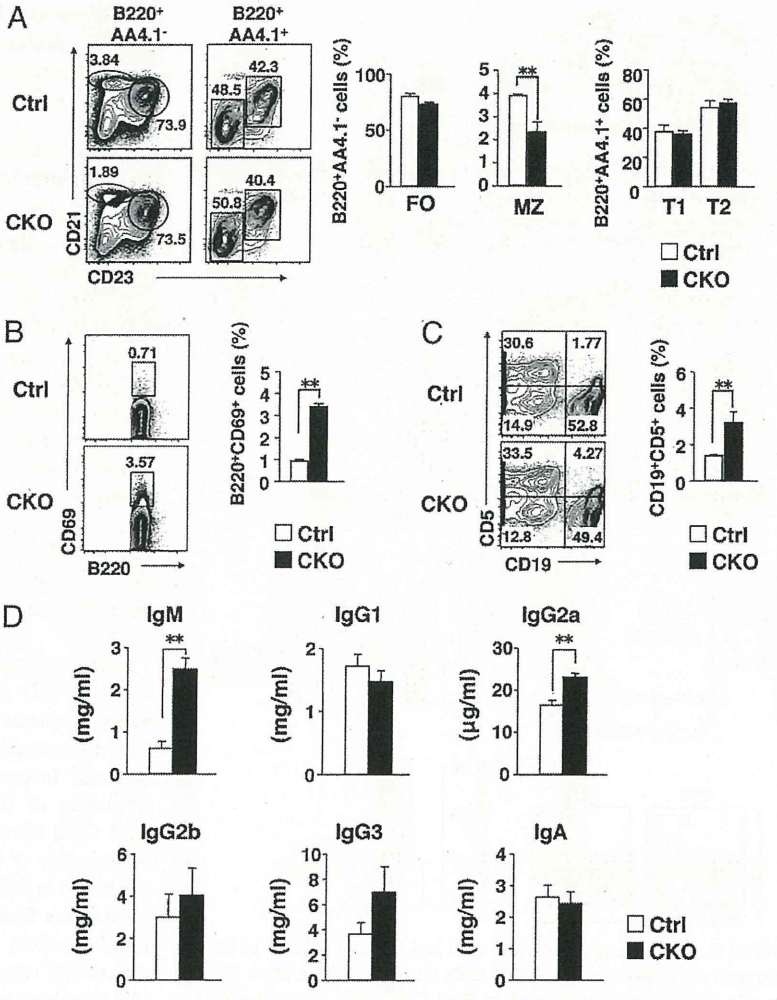

FIGURE 6. Analysis of B cell populations and serum Ig concentrations in Shp1 CKO mice. (**A**) Splenocytes from control or Shp1 CKO mice at 10–12 wk of age were stained for B220, AA4.1, CD21, and CD23 as well as with PI for analysis of follicular (FO) B ($CD21^{high}CD23^{high}$) and marginal-zone (MZ) B ($CD21^{high}CD23^{low}$) cells within the $B220^+AA4.1^-$-gated mature B cell population and of transitional T1 ($CD21^{high}CD23^{high}$) and T2 ($CD21^{low}CD23^{low}$) B cells within the $B220^+AA4.1^+$-gated immature B cells by flow cytometry (*left panel*). The percentage of MZ B cells or FO B cells among viable $B220^+AA4.1^-$ cells and that of T1 or T2 B cells among viable $B220^+AA4.1^+$ cells were determined (*middle* and *right panels*); data are means ± SE for three mice per group and are representative of two independent experiments. $^{**}p < 0.01$ (Student *t* test). (**B**) Splenocytes from control or Shp1 CKO mice at 10–12 wk of age were stained for B220 and CD69 as well as with PI for analysis of B220 and CD69 expression in all viable cells by flow cytometry. The percentage of activated B ($B220^+CD69^+$) cells among viable $B220^+$ cells was determined; data are means ± SE for three mice per group and are representative of two independent experiments. $^{**}p < 0.01$ (Student *t* test). (**C**) Splenocytes from control or Shp1 CKO mice at 10–12 wk of age were stained for CD19 and CD5 as well as with PI for analysis of CD19 and CD5 expression in viable cells by flow cytometry. The percentage of B-1a ($CD19^+CD5^+$) cells among all viable cells was determined; data are means ± SE for three mice per group and are representative of three independent experiments. $^{**}p < 0.01$ (Student *t* test). (**D**) Serum concentrations of IgM, IgG1, IgG2a, IgG2b, IgG3, and IgA in control or Shp1 CKO mice at 20–24 wk of age. Data are means ± SE for six mice per group and are representative of two independent experiments. $^{**}p < 0.01$ (Student *t* test).

serum creatinine in CKO mice were significantly higher than those of control mice (Fig. 7F). Moreover, the CKO mice had significantly higher serum titer of ANA as well as of IgG Abs to dsDNA compared with age-matched control mice (Fig. 7G).

Discussion

We have shown that Shp1 in $CD11c^+$ DCs is important for homeostatic regulation of both cDCs and pDCs in the spleen. The number of DN cDCs was markedly increased in the spleen of Shp1 CKO mice, whereas that of $CD4^+$ cDCs or $CD8^+$ cDCs was similar for Shp1 CKO and control mice. We also found that the incorporation rate of BrdU into splenic cDCs in the CKO mice was higher than that apparent with control mice (data not shown), suggesting that the proliferation and differentiation of cDCs likely increase in Shp1 CKO mice. All three subtypes of cDCs are thought to arise from the immediate precursors of cDCs, defined as lineage-negative $CD11c^+$MHC class II^-FLT3^+ cells (49). It is thus likely that Shp1 is required in a cell-autonomous manner for negative regulation of the development of cDCs, in particular that of DN cDCs, in the spleen. In contrast, an increase in the number of cDCs was not observed in either peripheral LNs or the thymus of Shp1 CKO mice, suggesting that the regulation of cDC homeostasis in the spleen differs from that in LNs and the thymus.

We have also shown that Shp1 is a negative regulator of multiple DC functions that are thought to be important for the promotion by DCs of the differentiation of naive T cells into Th cells. First, the migratory response of DCs to FITC painting was upregulated in Shp1 CKO mice, suggesting that Shp1 negatively regulates the ability of DCs to migrate to draining LNs after they have captured exogenous Ags. In addition, the expression level of CCR7 on $CD11c^+$ DCs was also upregulated in Shp1 CKO mice. Given that CCR7 is a receptor for CCL19 and CCL21, both of which promote DC migration (50), it is likely that Shp1 inhibits DC migration through downregulation of CCR7 expression. Second, expression of CD86, a costimulatory molecule that is important in the priming of naive T cells for their differentiation into Th cells, was also increased in $CD11c^+$ DCs of Shp1 CKO mice. Third, the LPS-induced production of proinflammatory cytokines such as TNF-α, IL-6, and IL-1β, which are implicated in the regulation of DC activity and of the differentiation of effector Th cells (2), was markedly increased in $CD11c^+$ DCs of Shp1 CKO mice.

Consistent with such enhanced activities of DCs in Shp1 CKO mice, the frequency of activated T cells, as well as that of IFN-γ–producing $CD4^+$ T cells, was increased in the spleen of the mutant animals. In contrast, the frequency of IL-17– or IL-4–producing $CD4^+$ T cells in the spleen was unaffected in Shp1 CKO mice. Moreover, the ability of $CD11c^+$ DCs from the spleen of Shp1 CKO mice to prime and induce Th1 (but not Th17) differentiation of OVA-specific $CD4^+$ T cells was enhanced. Shp1 in $CD11c^+$ DCs is thus important specifically for negative regulation of priming and Th1 differentiation of $CD4^+$ T cells by DCs. LPS-stimulated production of IL-12, a cytokine that is thought to be required for induction of Th1 cells from naive $CD4^+$ T cells, was markedly decreased in $CD11c^+$ DCs from Shp1 CKO mice, in-

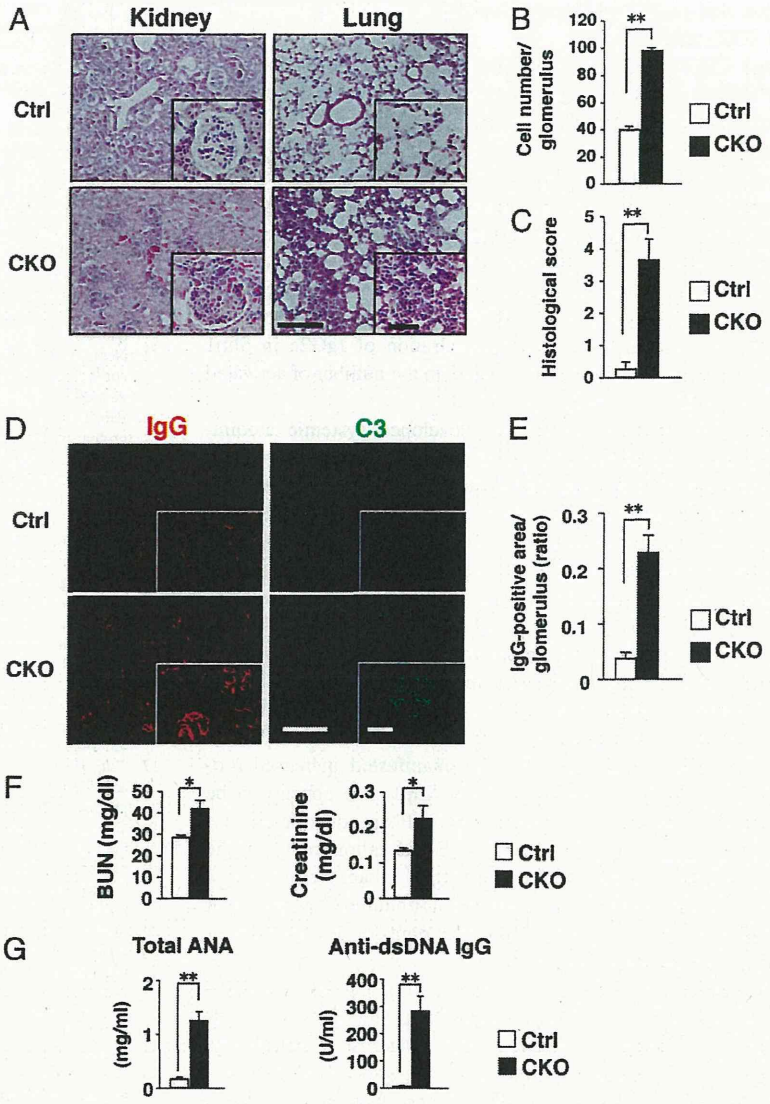

FIGURE 7. Development of autoimmunity in Shp1 CKO mice. (**A**) Paraffin-embedded sections of the kidney (*left panels*) and lung (*right panels*) from control or Shp1 CKO mice at 36–40 wk of age were stained with H&E. Images are representative of those from nine mice per group. *Insets* show higher magnification images of glomerulus and alveolar septa. Scale bars, 200 μm and 50 μm (*insets*). (**B**) For quantitative assessment of glomerular pathology, glomerular cellularity was examined by counting the number of cells with nuclei per each glomerulus. Twenty glomeruli of a similar size were examined for each animal. Data are means ± SE for a total of four mice per group. (**C**) Histological changes of the lung were also determined quantitatively by scoring of the following three categories (58): 1) interstitial infiltrates of lymphocytes and macrophages 2), perivascular infiltrates of lymphocytes and macrophages, and 3) expansion of BALT. Each category was scored as follows: 0, none; 1, mild; 2, moderate to severe. The sum of these scores thus represents the severity of inflammation with a maximum possible of 6. Data are means ± SE for a total of nine mice per group. $**p < 0.01$ (Student *t* test). (**D**) Frozen sections of the kidney from control or Shp1 CKO mice at 36–40 wk of age were subjected to immunohistofluorescence analysis of IgG (red) or C3 (green). *Insets* show higher magnification images of glomerulus. Scale bars, 200 μm and 50 μm (*insets*). Images are representative of those from nine (IgG) or three (C3) mice of each genotype. (**E**) A ratio of the IgG-positive area to that for a single glomerulus was determined by the use of ImageJ software. Data are means ± SE for 11 (control) and 15 (Shp1 CKO) glomeruli from total of three mice per group examined in three independent experiments. $**p < 0.01$ (Student *t* test). (**F**) Levels of blood urea nitrogen (BUN) and of serum creatinine in control or Shp1 CKO mice at 36–40 wk of age were determined. Data are means ± SE for eight mice per group. $*p < 0.05$ (Student *t* test). (**G**) Serum titers of total ANA and anti-dsDNA IgG in control or Shp1 CKO mice at 36–40 wk of age. Data are means ± SE for nine mice per group. $**p < 0.01$ (Student *t* test).

dicating that in contrast to other proinflammatory cytokines, the LPS-dependent production of IL-12 by CD11c$^+$ DCs is positively regulated by Shp1. This finding is consistent with the recent observation that bone marrow-derived macrophages prepared from *me^v/me^v* mice manifested marked impairment of LPS-induced IL-12 production (51). In contrast, Ramachandran et al. (22) reported that inhibition of Shp1 activity by a specific inhibitor of Shp1 increased the LPS-driven IL-12 production in bone marrow-derived DCs. Such difference may be attributable to that we or Zhou et al. (51) used isolated splenic DCs from Shp1 CKO mice or bone marrow-derived macrophages from *me^v/me^v* mice, respectively, whereas Ramachandran et al. (22) used bone marrow-derived DCs from wild-type mice. Thus, the reduced IL-12 production in Shp1 CKO or *me^v/me^v* mice may be, in part, an epiphenomenon due to disruption of splenic homeostasis in these mice. By contrast, expression of Delta 4 Notch-like ligand (52) or that of CD70 (53) on DCs is important for Th1 differentiation in a manner independent of IL-12. Indeed, we found that expression of CD70 on CD11c$^+$ DCs was markedly increased in the spleen of Shp1 CKO mice compared with control mice (data not shown). Thus, increased expression of CD70 on DCs might contribute to specific increase of Th1 differentiation in Shp1 CKO mice.

The molecular mechanism by which Shp1 negatively regulates the LPS-induced production of proinflammatory cytokines by CD11c$^+$ DCs remains largely unknown. However, we found that the enhancement of LPS-stimulated proinflammatory cytokine production apparent in DCs from Shp1 CKO mice was prevented by inhibitors of NF-κB activity, suggesting that Shp1 suppresses NF-κB–dependent signaling. In addition, Shp1 likely suppresses p38 MAPK- or JNK-dependent pathways in DCs. Moreover, the extent of tyrosine phosphorylation of proteins of ~70 and ~100 kDa was indeed increased in CD11c$^+$ DCs from the spleen of Shp1 CKO mice compared with that apparent for control mice. Characterization of these proteins as targets of the PTP activity of Shp1 in DCs may provide further insight into the molecular mechanism by which Shp1 negatively regulates DC functions.

DCs are also thought to play an important role in regulation of peripheral T cell tolerance through the production of IL-10 (3) as well as induction of Tregs (5, 6). However, the production of IL-10 in response to LPS was enhanced in isolated DCs from Shp1 CKO mice. In addition, the frequency of Tregs in the spleen was markedly increased in these animals. These results thus indicate that Shp1 in DCs is also a negative regulator of IL-10 production by DCs as well as of Treg homeostasis in the spleen. They further

suggest that peripheral T cell tolerance is not likely impaired in Shp1 CKO mice.

Shp1 CKO mice manifested increases both in the number of $CD5^+CD19^+$ (B-1a) cells in the spleen as well as in the concentrations of IgM and IgG2a in serum. Given that ~80% of IgM in serum is thought to be derived from B-1a cells (47), the increase in the serum level of IgM in Shp1 CKO mice is likely attributable in large part to the increase in the number of splenic B-1a cells. Shp1 in DCs is thus important for regulation of the homeostasis of B-1a cells in the spleen, although the molecular mechanism underlying such regulation remains unknown. In contrast, B cells are thought to secrete IgG2a in response to IFN-γ (54). It is therefore likely that the increase in the serum concentration of IgG2a in Shp1 CKO mice is attributable to the increase in the number of activated Th1 cells.

Shp1 CKO mice spontaneously developed systemic autoimmunity including glomerulonephritis and interstitial pneumonitis, with the former being associated with immune complex deposition in glomeruli. In addition, Shp1 CKO mice had markedly increased serum titers of autoantibodies such as ANA and anti-dsDNA. Defective regulation of either T cell immune responses or peripheral T cell tolerance by DCs is thought to give rise to autoimmunity (4, 10, 55). Our current results thus indicate that Shp1 in DCs plays an important role in protection against development of systemic autoimmunity, likely by limiting the development of Th1 cells. Moreover, development of SLE is thought to be attributable to activation of DCs in response to an excess of IFN-αβ (56). Given that DCs of Shp1 CKO mice manifested increased production of IFN-β in response to LPS, Shp1 also appears to be important for negative regulation of type I IFN production by DCs and consequent protection against SLE-like autoimmunity. The observation that me^v/me^v mice on the $Rag1^{-/-}$ background, which lack both T and B cells, also develop autoimmunity suggests that the loss of Shp1 in myeloid cells is important for development of autoimmunity in these mice (57).

In summary, we have shown that Shp1 negatively regulates various functions of DCs, in particular the promotion of Th1 cell differentiation, and that it thereby protects against autoimmunity. Development of an approach to activate Shp1 specifically in DCs may provide the basis for a potential new therapy for various autoimmune diseases.

Acknowledgments

We thank B.G. Neel and L.I. Pao for providing $Ptpn6^{fl/fl}$ mice, K. Okumura for the mAb to CD16/32, T. Hirano for OT-II mice, and H. Kobayashi, Y. Niwayama-Kusakari, E. Urano, and R. Koitabashi for technical assistance.

Disclosures

The authors have no financial conflicts of interest.

References

1. Steinman, R. M., and J. Banchereau. 2007. Taking dendritic cells into medicine. *Nature* 449: 419–426.
2. Coquerelle, C., and M. Moser. 2010. DC subsets in positive and negative regulation of immunity. *Immunol. Rev.* 234: 317–334.
3. Akbari, O., R. H. DeKruyff, and D. T. Umetsu. 2001. Pulmonary dendritic cells producing IL-10 mediate tolerance induced by respiratory exposure to antigen. *Nat. Immunol.* 2: 725–731.
4. Travis, M. A., B. Reizis, A. C. Melton, E. Masteller, Q. Tang, J. M. Proctor, Y. Wang, X. Bernstein, X. Huang, L. F. Reichardt, et al. 2007. Loss of integrin $\alpha(v)\beta_8$ on dendritic cells causes autoimmunity and colitis in mice. *Nature* 449: 361–365.
5. Mahnke, K., Y. Qian, J. Knop, and A. H. Enk. 2003. Induction of $CD4^+/CD25^+$ regulatory T cells by targeting of antigens to immature dendritic cells. *Blood* 101: 4862–4869.
6. Luo, X., K. V. Tarbell, H. Yang, K. Pothoven, S. L. Bailey, R. Ding, R. M. Steinman, and M. Suthanthiran. 2007. Dendritic cells with TGF-β1 differentiate naive $CD4^+CD25^-$ T cells into islet-protective $Foxp3^+$ regulatory T cells. *Proc. Natl. Acad. Sci. USA* 104: 2821–2826.
7. Hawiger, D., K. Inaba, Y. Dorsett, M. Guo, K. Mahnke, M. Rivera, J. V. Ravetch, R. M. Steinman, and M. C. Nussenzweig. 2001. Dendritic cells induce peripheral T cell unresponsiveness under steady state conditions in vivo. *J. Exp. Med.* 194: 769–779.
8. Probst, H. C., K. McCoy, T. Okazaki, T. Honjo, and M. van den Broek. 2005. Resting dendritic cells induce peripheral $CD8^+$ T cell tolerance through PD-1 and CTLA-4. *Nat. Immunol.* 6: 280–286.
9. Teichmann, L. L., M. L. Ols, M. Kashgarian, B. Reizis, D. H. Kaplan, and M. J. Shlomchik. 2010. Dendritic cells in lupus are not required for activation of T and B cells but promote their expansion, resulting in tissue damage. *Immunity* 33: 967–978.
10. Ohnmacht, C., A. Pullner, S. B. King, I. Drexler, S. Meier, T. Brocker, and D. Voehringer. 2009. Constitutive ablation of dendritic cells breaks self-tolerance of CD4 T cells and results in spontaneous fatal autoimmunity. *J. Exp. Med.* 206: 549–559.
11. Neel, B. G., H. Gu, and L. Pao. 2003. The 'Shp'ing news: SH2 domain-containing tyrosine phosphatases in cell signaling. *Trends Biochem. Sci.* 28: 284–293.
12. Pao, L. I., K. Badour, K. A. Siminovitch, and B. G. Neel. 2007. Nonreceptor protein-tyrosine phosphatases in immune cell signaling. *Annu. Rev. Immunol.* 25: 473–523.
13. Klingmüller, U., U. Lorenz, L. C. Cantley, B. G. Neel, and H. F. Lodish. 1995. Specific recruitment of SH-PTP1 to the erythropoietin receptor causes inactivation of JAK2 and termination of proliferative signals. *Cell* 80: 729–738.
14. Maeda, A., M. Kurosaki, M. Ono, T. Takai, and T. Kurosaki. 1998. Requirement of SH2-containing protein tyrosine phosphatases SHP-1 and SHP-2 for paired immunoglobulin-like receptor B (PIR-B)-mediated inhibitory signal. *J. Exp. Med.* 187: 1355–1360.
15. Matozaki, T., Y. Murata, H. Okazawa, and H. Ohnishi. 2009. Functions and molecular mechanisms of the CD47-SIRPalpha signalling pathway. *Trends Cell Biol.* 19: 72–80.
16. Shultz, L. D., P. A. Schweitzer, T. V. Rajan, T. Yi, J. N. Ihle, R. J. Matthews, M. L. Thomas, and D. R. Beier. 1993. Mutations at the murine motheaten locus are within the hematopoietic cell protein-tyrosine phosphatase (Hcph) gene. *Cell* 73: 1445–1454.
17. Tsui, H. W., K. A. Siminovitch, L. de Souza, and F. W. Tsui. 1993. Motheaten and viable motheaten mice have mutations in the haematopoietic cell phosphatase gene. *Nat. Genet.* 4: 124–129.
18. Green, M. C., and L. D. Shultz. 1975. Motheaten, an immunodeficient mutant of the mouse. I. Genetics and pathology. *J. Hered.* 66: 250–258.
19. Shultz, L. D., D. R. Coman, C. L. Bailey, W. G. Beamer, and C. L. Sidman. 1984. "Viable motheaten," a new allele at the motheaten locus. I. Pathology. *Am. J. Pathol.* 116: 179–192.
20. Shultz, L. D. 1988. Pleiotropic effects of deleterious alleles at the "motheaten" locus. *Curr. Top. Microbiol. Immunol.* 137: 216–222.
21. Nakayama, K., K. Takahashi, L. D. Shultz, K. Miyakawa, and K. Tomita. 1997. Abnormal development and differentiation of macrophages and dendritic cells in viable motheaten mutant mice deficient in haematopoietic cell phosphatase. *Int. J. Exp. Pathol.* 78: 245–257.
22. Ramachandran, I. R., W. Song, N. Lapteva, M. Seethammagari, K. M. Slawin, D. M. Spencer, and J. M. Levitt. 2011. The phosphatase SRC homology region 2 domain-containing phosphatase-1 is an intrinsic central regulator of dendritic cell function. *J. Immunol.* 186: 3934–3945.
23. Caton, M. L., M. R. Smith-Raska, and B. Reizis. 2007. Notch-RBP-J signaling controls the homeostasis of $CD8^-$ dendritic cells in the spleen. *J. Exp. Med.* 204: 1653–1664.
24. Pao, L. I., K. P. Lam, J. M. Henderson, J. L. Kutok, M. Alimzhanov, L. Nitschke, M. L. Thomas, B. G. Neel, and K. Rajewsky. 2007. B cell-specific deletion of protein-tyrosine phosphatase Shp1 promotes B-1a cell development and causes systemic autoimmunity. *Immunity* 27: 35–48.
25. Barnden, M. J., J. Allison, W. R. Heath, and F. R. Carbone. 1998. Defective TCR expression in transgenic mice constructed using cDNA-based α- and β-chain genes under the control of heterologous regulatory elements. *Immunol. Cell Biol.* 76: 34–40.
26. Tomizawa, T., Y. Kaneko, Y. Kaneko, Y. Saito, H. Ohnishi, J. Okajo, C. Okuzawa, T. Ishikawa-Sekigami, Y. Murata, H. Okazawa, et al. 2007. Resistance to experimental autoimmune encephalomyelitis and impaired T cell priming by dendritic cells in Src homology 2 domain-containing protein tyrosine phosphatase substrate-1 mutant mice. *J. Immunol.* 179: 869–877.
27. Saito, Y., H. Iwamura, T. Kaneko, H. Ohnishi, Y. Murata, H. Okazawa, Y. Kanazawa, M. Sato-Hashimoto, H. Kobayashi, P. A. Oldenborg, et al. 2010. Regulation by SIRPα of dendritic cell homeostasis in lymphoid tissues. *Blood* 116: 3517–3525.
28. Iwamura, H., Y. Saito, M. Sato-Hashimoto, H. Ohnishi, Y. Murata, H. Okazawa, Y. Kanazawa, T. Kaneko, S. Kusakari, T. Kotani, et al. 2011. Essential roles of SIRPα in homeostatic regulation of skin dendritic cells. *Immunol. Lett.* 135: 100–107.
29. Kanazawa, Y., Y. Saito, Y. Supriatna, H. Tezuka, T. Kotani, Y. Murata, H. Okazawa, H. Ohnishi, Y. Kinouchi, Y. Nojima, et al. 2010. Role of SIRPα in regulation of mucosal immunity in the intestine. *Genes Cells* 15: 1189–1200.
30. Shortman, K., and S. H. Naik. 2007. Steady-state and inflammatory dendritic-cell development. *Nat. Rev. Immunol.* 7: 19–30.
31. Hou, B., B. Reizis, and A. L. DeFranco. 2008. Toll-like receptors activate innate and adaptive immunity by using dendritic cell-intrinsic and -extrinsic mechanisms. *Immunity* 29: 272–282.

32. Melillo, J. A., L. Song, G. Bhagat, A. B. Blazquez, C. R. Plumlee, C. Lee, C. Berin, B. Reizis, and C. Schindler. 2010. Dendritic cell (DC)-specific targeting reveals Stat3 as a negative regulator of DC function. *J. Immunol.* 184: 2638–2645.
33. Vremec, D., J. Pooley, H. Hochrein, L. Wu, and K. Shortman. 2000. CD4 and CD8 expression by dendritic cell subtypes in mouse thymus and spleen. *J. Immunol.* 164: 2978–2986.
34. Wu, L., and Y. J. Liu. 2007. Development of dendritic-cell lineages. *Immunity* 26: 741–750.
35. Leenen, P. J., K. Radosević, J. S. Voerman, B. Salomon, N. van Rooijen, D. Klatzmann, and W. van Ewijk. 1998. Heterogeneity of mouse spleen dendritic cells: in vivo phagocytic activity, expression of macrophage markers, and subpopulation turnover. *J. Immunol.* 160: 2166–2173.
36. Zietara, N., M. Łyszkiewicz, N. Gekara, J. Puchałka, V. A. Dos Santos, C. R. Hunt, T. K. Pandita, S. Lienenklaus, and S. Weiss. 2009. Absence of IFN-β impairs antigen presentation capacity of splenic dendritic cells via down-regulation of heat shock protein 70. *J. Immunol.* 183: 1099–1109.
37. Merad, M., F. Ginhoux, and M. Collin. 2008. Origin, homeostasis and function of Langerhans cells and other langerin-expressing dendritic cells. *Nat. Rev. Immunol.* 8: 935–947.
38. Liu, K., and M. C. Nussenzweig. 2010. Origin and development of dendritic cells. *Immunol. Rev.* 234: 45–54.
39. Miyake, A., Y. Murata, H. Okazawa, H. Ikeda, Y. Niwayama, H. Ohnishi, Y. Hirata, and T. Matozaki. 2008. Negative regulation by SHPS-1 of Toll-like receptor-dependent proinflammatory cytokine production in macrophages. *Genes Cells* 13: 209–219.
40. Kawai, T., and S. Akira. 2011. Toll-like receptors and their crosstalk with other innate receptors in infection and immunity. *Immunity* 34: 637–650.
41. Cuzzocrea, S., P. K. Chatterjee, E. Mazzon, L. Dugo, I. Serraino, D. Britti, G. Mazzullo, A. P. Caputi, and C. Thiemermann. 2002. Pyrrolidine dithiocarbamate attenuates the development of acute and chronic inflammation. *Br. J. Pharmacol.* 135: 496–510.
42. Shin, H. M., M. H. Kim, B. H. Kim, S. H. Jung, Y. S. Kim, H. J. Park, J. T. Hong, K. R. Min, and Y. Kim. 2004. Inhibitory action of novel aromatic diamine compound on lipopolysaccharide-induced nuclear translocation of NF-kappaB without affecting IkappaB degradation. *FEBS Lett.* 571: 50–54.
43. Dillon, S. R., C. Sprecher, A. Hammond, J. Bilsborough, M. Rosenfeld-Franklin, S. R. Presnell, H. S. Haugen, M. Maurer, B. Harder, J. Johnston, et al. 2004. Interleukin 31, a cytokine produced by activated T cells, induces dermatitis in mice. *Nat. Immunol.* 5: 752–760.
44. Steinman, R. M., D. Hawiger, and M. C. Nussenzweig. 2003. Tolerogenic dendritic cells. *Annu. Rev. Immunol.* 21: 685–711.
45. Jang, I. K., D. G. Cronshaw, L. K. Xie, G. Fang, J. Zhang, H. Oh, Y. X. Fu, H. Gu, and Y. Zou. 2011. Growth-factor receptor-bound protein-2 (Grb2) signaling in B cells controls lymphoid follicle organization and germinal center reaction. *Proc. Natl. Acad. Sci. USA* 108: 7926–7931.
46. Atencio, S., H. Amano, S. Izui, and B. L. Kotzin. 2004. Separation of the New Zealand Black genetic contribution to lupus from New Zealand Black determined expansions of marginal zone B and B1a cells. *J. Immunol.* 172: 4159–4166.
47. Baumgarth, N. 2011. The double life of a B-1 cell: self-reactivity selects for protective effector functions. *Nat. Rev. Immunol.* 11: 34–46.
48. Mackay, F., P. A. Silveira, and R. Brink. 2007. B cells and the BAFF/APRIL axis: fast-forward on autoimmunity and signaling. *Curr. Opin. Immunol.* 19: 327–336.
49. Liu, K., G. D. Victora, T. A. Schwickert, P. Guermonprez, M. M. Meredith, K. Yao, F. F. Chu, G. J. Randolph, A. Y. Rudensky, and M. Nussenzweig. 2009. In vivo analysis of dendritic cell development and homeostasis. *Science* 324: 392–397.
50. Förster, R., A. Schubel, D. Breitfeld, E. Kremmer, I. Renner-Müller, E. Wolf, and M. Lipp. 1999. CCR7 coordinates the primary immune response by establishing functional microenvironments in secondary lymphoid organs. *Cell* 99: 23–33.
51. Zhou, D., C. A. Collins, P. Wu, and E. J. Brown. 2010. Protein tyrosine phosphatase SHP-1 positively regulates TLR-induced IL-12p40 production in macrophages through inhibition of phosphatidylinositol 3-kinase. *J. Leukoc. Biol.* 87: 845–855.
52. Skokos, D., and M. C. Nussenzweig. 2007. $CD8^-$ DCs induce IL-12-independent Th1 differentiation through Delta 4 Notch-like ligand in response to bacterial LPS. *J. Exp. Med.* 204: 1525–1531.
53. Soares, H., H. Waechter, N. Glaichenhaus, E. Mougneau, H. Yagita, O. Mizenina, D. Dudziak, M. C. Nussenzweig, and R. M. Steinman. 2007. A subset of dendritic cells induces $CD4^+$ T cells to produce IFN-γ by an IL-12-independent but CD70-dependent mechanism in vivo. *J. Exp. Med.* 204: 1095–1106.
54. Snapper, C. M., and W. E. Paul. 1987. Interferon-γ and B cell stimulatory factor-1 reciprocally regulate Ig isotype production. *Science* 236: 944–947.
55. Chen, M., Y. H. Wang, Y. Wang, L. Huang, H. Sandoval, Y. J. Liu, and J. Wang. 2006. Dendritic cell apoptosis in the maintenance of immune tolerance. *Science* 311: 1160–1164.
56. Banchereau, J., V. Pascual, and A. K. Palucka. 2004. Autoimmunity through cytokine-induced dendritic cell activation. *Immunity* 20: 539–550.
57. Yu, C. C., H. W. Tsui, B. Y. Ngan, M. J. Shulman, G. E. Wu, and F. W. Tsui. 1996. B and T cells are not required for the viable motheaten phenotype. *J. Exp. Med.* 183: 371–380.
58. Mankowski, J. L., D. L. Carter, J. P. Spelman, M. L. Nealen, K. R. Maughan, L. M. Kirstein, P. J. Didier, R. J. Adams, M. Murphey-Corb, and M. C. Zink. 1998. Pathogenesis of simian immunodeficiency virus pneumonia: an immunopathological response to virus. *Am. J. Pathol.* 153: 1123–1130.

Regular Article

HEMATOPOIESIS AND STEM CELLS

Polymorphic *Sirpa* is the genetic determinant for NOD-based mouse lines to achieve efficient human cell engraftment

Takuji Yamauchi,[1] Katsuto Takenaka,[1] Shingo Urata,[1] Takahiro Shima,[1] Yoshikane Kikushige,[1] Takahito Tokuyama,[1] Chika Iwamoto,[1] Mariko Nishihara,[1] Hiromi Iwasaki,[2] Toshihiro Miyamoto,[1] Nakayuki Honma,[3] Miki Nakao,[4] Takashi Matozaki,[5] and Koichi Akashi[1,2]

[1]Department of Medicine and Biosystemic Science, Kyushu University Graduate School of Medical Sciences, Fukuoka, Japan; [2]Center for Cellular and Molecular Medicine, Kyushu University Hospital, Fukuoka, Japan; [3]Innovative Drug Research Laboratories, Kyowa Hakko Kirin Co Ltd, Tokyo, Japan; [4]Department of Bioscience and Biotechnology, Graduate School of Bioresource and Bioenvironmental Sciences, Kyushu University, Fukuoka, Japan; and [5]Division of Molecular and Cellular Signaling, Department of Biochemistry and Molecular Biology, Kobe University Graduate School of Medicine, Kobe, Japan

Key Points

- NOD-specific *Sirpa* polymorphism is the genetic determinant of highly efficient xenograft activity in NOD-based immunodeficient mouse models.

Current mouse lines efficient for human cell xenotransplantation are backcrossed into NOD mice to introduce its multiple immunodeficient phenotypes. Our positional genetic study has located the NOD-specific polymorphic *Sirpa* as a molecule responsible for its high xenograft efficiency: it recognizes human CD47 and the resultant signaling may cause NOD macrophages not to engulf human grafts. In the present study, we established C57BL/6.*Rag2*^{null}*Il2rg*^{null} mice harboring NOD-*Sirpa* (BRGS). BRGS mice engrafted human hematopoiesis with an efficiency that was equal to or even better than that of the NOD.*Rag1*^{null}*Il2rg*^{null} strain, one of the best xenograft models. Consequently, BRGS mice are free from other NOD-related abnormalities; for example, they have normalized C5 function that enables the evaluation of complement-dependent cytotoxicity of antibodies against human grafts in the humanized mouse model. Our data show that efficient human cell engraftment found in NOD-based models is mounted solely by their polymorphic *Sirpa*. The simplified BRGS line should be very useful in future studies of human stem cell biology. (*Blood*. 2013;121(8):1316-1325)

Introduction

Immunodeficient mice are widely used to reconstitute human hematopoiesis by xenotransplantation of hematopoietic stem cells (HSCs).[1,2] This "humanized" mouse model provides a powerful tool with which to evaluate the biologic properties of human HSCs and progenitors in vivo.[3,4] Such xenotransplantation systems have also been used to study human cancer stem cells.[5-8]

Elimination of the lymphoid system is the first step to achieving reconstitution of human hematopoiesis. To deplete T and B cells, the *scid* mutation in the *Prkdc* gene[9-11] or disruption of the recombination activating gene 1 or 2 (*Rag1* and *Rag2*)[12,13] has been introduced into various mouse strains. In addition, to deplete natural killer (NK) cells or their functions, the IL-2 receptor common γ chain subunit (*Il2rg*)[14-16] or beta-2-microglobulin (*B2m*)[17-19] is disrupted.

However, depletion of lymphoid cells is not sufficient and it has been shown empirically that additional strain-specific factors modulate human hematopoietic engraftment in the xenotransplantation setting. For example, within the SCID strain, the SCID with the NOD background was the gold standard for the xenotransplantation assay based on its high efficiency.[11] In fact, recent studies have shown that among the lymphoid-depleted mouse strains, the NOD-*scid* *Il2rg*^{null} (NSG/NOG)[14,15] and NOD.*Rag1*^{null}*Il2rg*^{null} (NOD-RG)[20] strains are the most efficient; the BALB/c.*Rag2*^{null}*Il2rg*^{null} (BALB-RG) strain is the next efficient[21,22]; and the C57BL/6 strains with *scid*,[23] *Rag2*^{null}, *Rag2*^{null}*B2m*^{null}, *Rag2*^{null}*Prf*^{null},[24] or *Rag2*^{null}*Jak3*^{null}[25] mutations are unable to reconstitute human hematopoiesis. The NOD strain has multiple immune deficiencies, including defects of appropriate regulation of the T-lymphocyte repertoire, antigen presenting cell function, NK cell function,[26]and hemolytic complement (C5) and cytokine production from macrophages,[27] and these abnormalities are presumed to collaborate to cause the development of autoimmune diabetes and hemolytic anemia.[26,28] To establish xenotransplantation models, lymphoid-depleted strains have been backcrossed into the NOD/ShiLt–inbred strain multiple times to introduce such numerous NOD-specific abnormalities.[14,15] However, it was unknown whether we could select a genetic determinant(s) specially required to achieve the NOD-specific high engraftment capability for human cells.

Previously, we used positional genetics to characterize the molecular basis for this capability in the NOD strain by measuring the ability of mouse BM stromal layers to support hematopoietic long-term culture-initiating cell activity (LTC-IC) in vitro and identified the strain differences as the polymorphism of the *Sirpa* gene located within the insulin-dependent diabetes (*Idd-13*) locus.[24]

Submitted June 28, 2012; accepted December 9, 2012. Prepublished online as *lood* First Edition paper, January 4, 2013; DOI 10.1182/blood-2012-06-440354.

The online version of this article contains a data supplement.

The publication costs of this article were defrayed in part by page charge payment. Therefore, and solely to indicate this fact, this article is hereby marked "advertisement" in accordance with 18 USC section 1734.

Stroma cells from the NOD BM supports LTC-IC of human cells, but those from C57BL/6 could not. Enforced expression of the NOD-type SIRPA enabled C57BL/6 stroma cells to support human LTC-IC.[24] This in vitro finding is also applicable to the in vivo setting, as shown by another study in which a human *SIRPA* BAC transgene introduced into *Rag2*^{null}*Il2rg*^{null} mice on a mixed 129; BALB/c background significantly improved the efficiency of human hematopoietic engraftment.[29]

SIRPA is a transmembrane protein that contains 3 Ig-like domains within the extracellular region. It is expressed in macrophages, myeloid cells, and neurons, and interacts with its ligand CD47 through its respective IgV-like domains, where the NOD strain has specific polymorphism. CD47 is a member of the Ig superfamily that is ubiquitously expressed in hematopoietic and nonhematopoietic cells. The cytoplasmic region of SIRPA has immunoreceptor tyrosine–based inhibitory motifs, and binding cell-surface CD47 with SIRPA on macrophages provokes inhibitory signals through phosphorylation of these inhibitory motifs of SIRPA,[30] preventing their phagocytic activity.[31-33] A recent study also showed that transgenic expression of mouse CD47 into CD34$^+$CD38$^-$ human fetal liver cells significantly enhanced the human cell engraftment into BALB-RG mice.[34] Based on these data, the binding of NOD-SIRPA with human CD47 might produce signals for mouse macrophages not to engulf human HSCs, which presumably makes the strain permissive for human HSC engraftment.[24]

The most important question was whether the NOD-specific highly efficient human cell engraftment in vivo could be explained solely by the NOD-*Sirpa* polymorphism. In the present study, we established a C57BL/6.*Rag2*^{null}*Il2rg*^{null} (C57BL/6-RG) mouse line harboring the NOD-type *Sirpa*. Our data show clearly that replacement of the C57BL/6-type *Sirpa* with the NOD-type *Sirpa* is sufficient for the C57BL/6-RG strain to be endowed with the xenotransplantation capability that is at least equal to NOD-RG mice. Therefore, we successfully segregated the genetic abnormality responsible for efficient human cell engraftment from multiple genetic abnormalities in the NOD strain. The simplified humanized mouse system established by the new C57BL/6.*Rag2*^{null}*Il2rg*^{null}NOD-*Sirpa* (BRGS) strain should be very useful in improving xenotransplantation strategies in future studies of human cell biology.

Methods

Mice

C57BL/6, C57BL/6.NOD-*Idd13*, NOD, NOD.CB17-*Prkdc*^{scid} (NOD-*scid*), and NOD.Cg-*Rag1*^{tm1Mom}*Il2rg*^{tm1Wjl}/Sz (NOD-RG) mice were purchased from the Jackson Laboratory; C57BL/6.*Rag2*^{tm1Fwa}*Il2rg*^{tm1Wjl} (C57BL/6-RG) mice were purchased from Taconic. All mice were bred and maintained in individual ventilated cages at the Kyushu University Animal Facility and fed with autoclaved food and water. BRGS mice were generated by breeding C57BL/6-RG and C57BL/6.NOD-*Idd13* mice and backcrossed with C57BL/6-RG mice. *Rag2* gene and *Sirpa* gene are located on chromosome 2 with 17.1 cM. First, we repeated the breeding of C57BL/6-RG and C57BL/6.NOD-*Idd13* mice, and after 10 breedings, we obtained the recombination between the *Rag2*$^-$ and the *Sirpa*^{NOD} loci by chromosomal crossover. This was examined by genotyping by the microsatellite markers *D2Mit447* and *D2Mit338*, which are 0.63 cM apart on chromosome 2, during interbreeding. In addition, *Sirpa, Rag2*, and *Il2rg* were genetically typed by PCR and direct sequencing. In C57BL/6.NOD-(*D2Mit447-D2Mit338*) *Rag2*^{null}*Il2rg*^{null} mice, the region between *D2Mit447* and *D2Mit338* contains 33 genes, including *Sirpa*, but *Sirpa* is the only gene within the *Idd13* locus that is expressed in BM stromal cells and macrophages and had coding sequence polymorphism between the NOD and other strains.[24] Therefore, we refer to our established mouse line as BRGS herein. Sequences of the oligonucleotide primers used are provided in supplemental Table 1 (available on the *Blood* Web site; see the Supplemental Materials link at the top of the online article). All experiments were conducted following the guidelines of the institutional animal committee of Kyushu University.

Binding affinity of mouse macrophages to human CD47-Fc

Mouse macrophages were obtained by peritoneal lavage. Cells were stained with purified anti–mouse Sirpa (P84; BD Biosciences) conjugated with PE and anti–mouse CD11b (3A33; Beckman Coulter) conjugated with FITC. CD11b$^+$SIRPA$^+$ cells were defined as mature macrophages. The binding between SIRPA and CD47 was assessed by staining with biotinylated human CD47-Fc conjugated with streptavidin-allophycocyanin (APC),[35] and analyzed with a FACSAria III cell sorter (BD Biosciences).

In vitro mouse macrophage phagocytosis assays for human hematopoietic stem cells

Phagocytic activity of mouse macrophages against the human CD34$^+$CD38$^-$ population that contains the majority of human HSCs was evaluated in vitro, as described previously.[36] In brief, mouse peritoneal-derived macrophages were incubated at 1.0×10^4 cells in 200 μL of RPMI 1640 medium in Falcon culture tubes (2058; BD Biosciences). Cells were opsonized with CD34 antibody (sc-19621; Santa Cruz Biotechnology), incubated with mouse IFN-γ (100 ng/mL; R&D Systems) for 24 hours, and then lipopolysaccharide (0.3 μg/μL) for 1 hour. Human cord blood (CB) HSCs were then added to the tubes. Two hours after coincubation with macrophages and target cells, the phagocytic index was calculated using the following formula: phagocytic index = number of ingested cells/(number of macrophages/100). At least 200 macrophages were counted by a blinded observer.

Sensitivity of BRGS mice to irradiation

Cohorts of BRGS mice were exposed to varying doses of the whole-body irradiation from a ^{137}Cs γ-irradiator. The mice were examined daily and euthanized when moribund. Surviving mice were euthanized at 8 weeks after irradiation. NOG/NSG mice are highly radiosensitive because of the *scid* mutation. To examine the radiosensitivity of BRGS mice, 6- to 10-week-old BRGS mice were irradiated with 550-670 cGy, and monitored for 8 weeks. Early deaths were observed in the mouse group irradiated with more than 620 cGy, whereas those irradiated with 550-580 cGy survived at the end of 8 weeks. Based on these data, we irradiated BRGS mice at 580 cGy in all xenotransplantation experiments. The irradiation doses for experiments with NOD-RG (420 cGy) and C57BL/6-RG (670 cGy) were decided by radiosensitivity experiments.

Transplantation of human HSCs into mice

CB cells were collected during normal full-term deliveries after obtaining informed consent in accordance with the Declaration of Helsinki (provided by the Kyushu Block Red Cross Blood Center, Japan Red Cross Society). Mononuclear cells were separated by Ficoll-Hypaque density-gradient centrifugation. Lineage-depleted CB cells were obtained magnetically using a lineage cell depletion kit (Miltenyi Biotec). A total of 5×10^3 CD34$^+$CD38$^-$ cells were injected intrafemorally into mice. Within an individual experiment, mice of each strain received CD34$^+$CD38$^-$ cells purified from the same mixture of CB cells from multiple donors. After transplantation, mice were given sterile water containing prophylactic enrofloxacin (Baytril; Bayer HealthCare). Mice were killed 8, 16, or 24 weeks after transplantation.

Antibodies, cell staining, and sorting

For the analyses of mouse T, B, and NK cells, mouse peripheral blood cells were stained with PE-conjugated anti-CD3 (145-2C11), FITC-conjugated

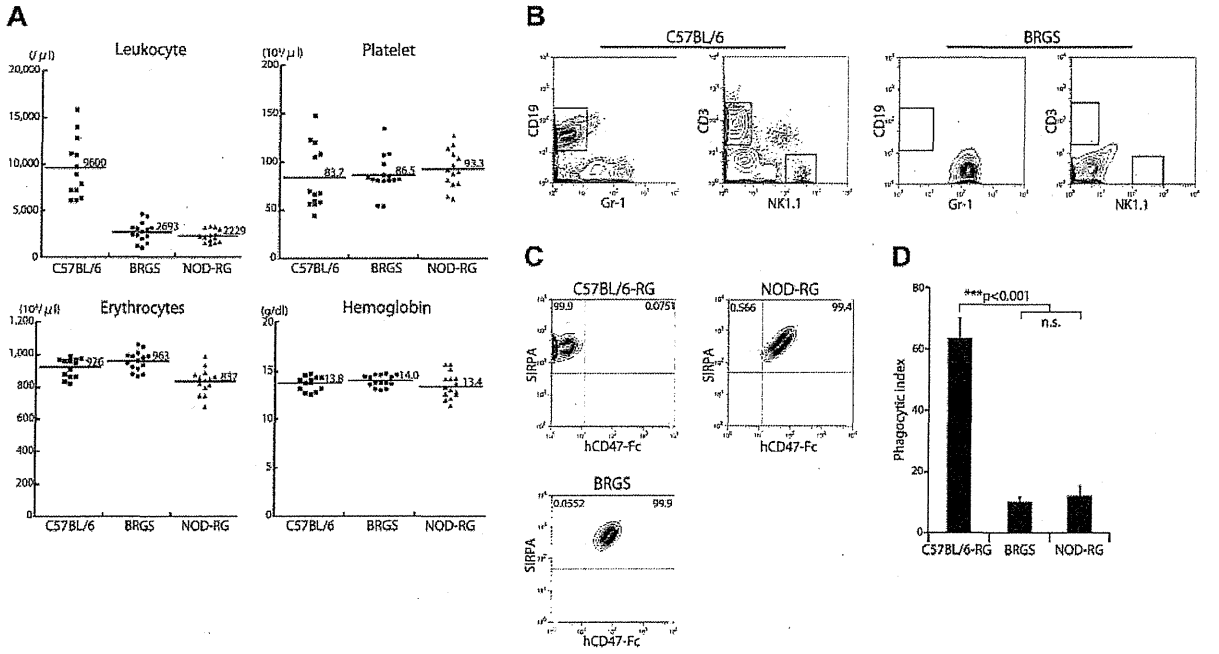

Figure 1. BRGS mice lack lymphocytes and SIRPA recognizes human CD47-Fc. (A) Frequencies of blood leukocytes, erythrocytes, hemoglobin, and platelets in BRGS mice. Leukocyte counts in BRGS ($2.69 \pm 1.01 \times 10^3/\mu L$) and NOD-RG mice ($2.23 \pm 0.7 \times 10^3/\mu L$) are significantly decreased compared with that in C57BL/6 mice ($9.6 \pm 0.32 \times 10^3/\mu L$). BRGS mice have normal erythrocyte ($9.63 \pm 0.63 \times 10^6/\mu L$), hemoglobin ($14.0 \pm 0.6$ g/dL), and platelet ($8.7 \pm 2.0 \times 10^5/\mu L$) counts. (B) Representative FACS plots of blood in C57BL/6 and BRGS mice. BRGS mice lacked T, B, and NK cells. (C) Binding activity of human CD47-Fc to SIRPA expressed in peritoneal macrophages derived from C57BL/6-RG, BRGS, or NOD-RG mice. Macrophages from BRGS and NOD-RG mice, but not those from C57BL/6-RG mice, were stained with human CD47-Fc on FACS. (D) Phagocytosis assay of C57BL/6-RG, BRGS, or NOD-RG macrophages against human $CD34^+CD38^-$ CB HSCs ($n = 3$). The phagocytic index was determined as the number of engulfed cells per 100 macrophages. Bars indicate mean ± SD.

anti-CD19 (1D3), APC-conjugated anti-NK1.1 (PK136; BD Biosciences), and Pacific Blue–conjugated anti–Gr-1 (RB6-8C5; BioLegend). Sorting of $CD34^+CD38^-$ subfractions was accomplished by staining lineage-depleted CB cells with FITC-conjugated anti-CD34 (581/CD34) and PE-conjugated anti-CD38 (HIT2; BD Biosciences). For analysis and sorting of human cells in the immunodeficient mice, FITC-conjugated anti-CD4 (RPA-T4), CD33 (HIM3-4), CD41a (HIP8), TCR αβ (WT31), TCR γδ (11F2), Igλ L chain (JDC-12), Igκ L chain (G20-193; BD Biosciences), anti-CD10 (SS2/36; Dako), PE-conjugated anti-CD8 (RPA-T8), CD20 (2H7), NKp46 (9E2; BD Biosciences), CD235a (JC159; Dako), PE-Cy7–conjugated anti-CD3 (SK7; BD Biosciences), CD19 (HIB19; BioLegend), APC-conjugated anti-CD45 (J33; Beckman Coulter), and PaB-conjugated anti–mouse CD45 (30-F11; BioLegend) monoclonal antibodies were used in addition to the antibodies described in the preceding paragraph. Nonviable cells were excluded by propidium iodide staining. The cells were analyzed and sorted with a FACSAria cell sorter (BD Biosciences).

Complement-dependent hemolytic activity

To estimate the serum complement activity of mice, the peripheral blood of mice were collected in 1.5-mL tubes and allowed to stand at room temperature for 1 hour. The serum was collected after centrifugation of the blood at 200*g* for 15 minutes at 4°C and stored −80°C until use. The mixtures of each diluted sera of mice, 3.75×10^6 erythrocytes of sheep and 2.5μg of zymosan (Imgenex) were incubated 10 hours at 37°C. After incubation, the absorbance of each sample at 415 nm was measured.

In vivo antibody treatment in a disseminated lymphoma xenograft model

A total of 8×10^5 Raji cells (Burkitt lymphoma cell line; American Type Culture Collection) were injected into BRGS or NOD-RG mice (6-10 weeks of age) via the tail vein. Raji cells proliferated predominantly in the BM. Ten days after injection, these mice were IP injected daily with 200 μg of rituximab or mouse IgG2a control for 1 week and then BM cells were collected and analyzed with the FACSAria III.

Statistical analysis

Data are presented as means ± SD. The significance of the differences between groups was determined via the Student *t* test. For comparison of complement-dependent hemolytic activity among the mouse strains, repeated-measures ANOVA was performed.

Results

Establishment of the BRGS mouse

The BRGS mouse line was established by breeding the C57BL/6-RG with the C57BL/6.NOD-*Idd13* mouse that is congenic for NOD-derived *Idd13* locus within which the *Sirpa* is the only gene that is polymorphic and is expressed in the BM stromal cells.[24] BRGS mice were all born healthy and displayed good fertility. They showed a median life span of 65 weeks without the development of lymphoma that usually occurs in the NOD-*scid* strain after the age of > 5 months.[11]

As shown in Figure 1A, BRGS mice had normal levels of hemoglobin and platelets, but a low number of leukocytes. This is because of the lack of $CD3^+$ T cells, $CD19^+$ B cells, and $NK1.1^+$ NK cells (Figure 1B). IP macrophages from either C57BL/6-RG, BRGS or NOD-RG mice were evaluated for the binding to human CD47 on FACS. $CD11b^+$ peritoneal macrophages strongly expressed SIRPA in all of these strains. As shown in Figure 1C, both macrophages from the BRGS and those from the NOD-RG strain bound to the human CD47-Fc protein, whereas those from the

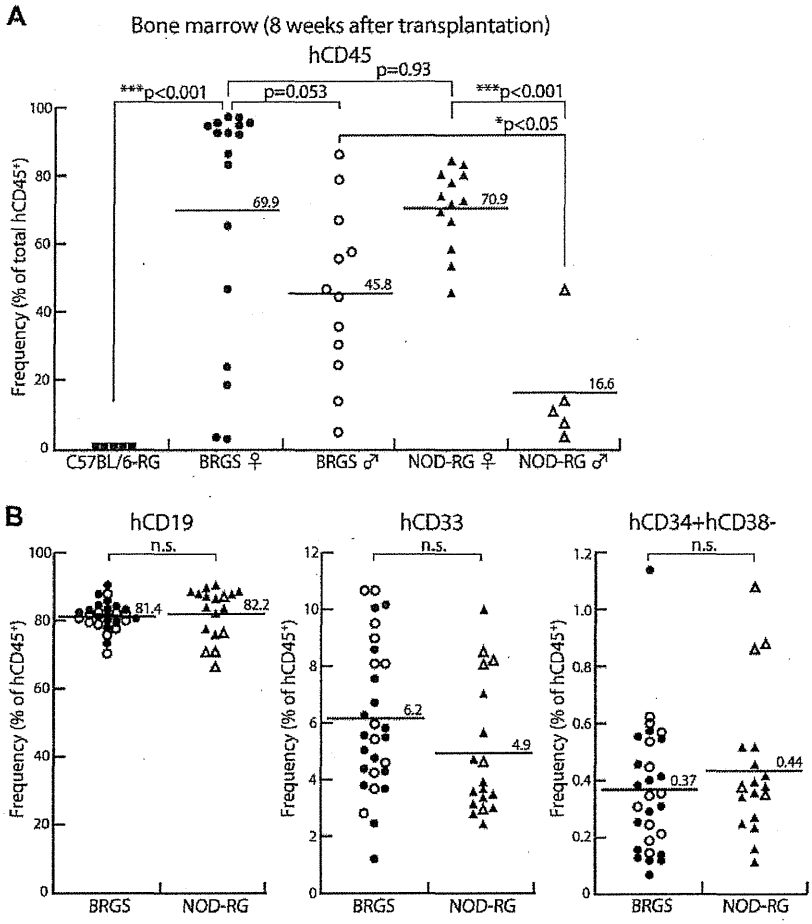

Figure 2. BRGS mice show efficient engraftment of human HSCs comparable to NOD-RG mice. In the BM, human HSC engraftment was examined by flow cytometric analysis 8 weeks after transplantation. C57BL/6-RG mice (■; n = 5), female BRGS mice (●; n = 17), male BRGS mice (○; n = 12), female NOD-RG mice (▲; n = 13), and male NOD-RG mice (△; n = 5) mice were analyzed. (A) Both BRGS and NOD-RG female mice showed excellent human CD45$^+$ reconstitution. BRGS male mice showed significantly better engraftment compared with NOD-RG male mice. (B) Frequencies of CD19$^+$ B cells, CD33$^+$ myeloid cells, and CD34$^+$CD38$^-$ HSCs in BRGS and NOD-RG mice.

C57BL/6 strain did not, confirming that BRGS mice have the NOD-type SIRPA that can bind to human CD47. Consistent with these binding data, when macrophages of each strain were cultured with human CD34$^+$CD38$^-$ cells, macrophages from C57BL/6-RG mice, but not those from BRGS or NOD-RG mice, actively engulfed human CD34$^+$CD38$^-$ cells, as shown by the significant elevation of the phagocytic index in the C57BL/6-RG mice (Figure 1D).

BRGS mice are capable of multilineage reconstitution of human hematopoiesis with efficiency at least equal to that of NOD-RG mice

A recent study has shown that intrafemoral injection is more efficient than IV injection in the xenotransplantation setting.[37] We used intrafemoral injection into adult mice in the present study because our preliminary data also showed that human cell chimerisms of adult BRGS by intrafemoral injection was significantly better than those with IV injection (data not shown). We transplanted 5×10^3 CD34$^+$CD38$^-$ human CB cells intrafemorally into C57BL/6-RG, BRGS or NOD-RG mice at the age of 6-8 weeks. Before transplantation, C57BL/6-RG, BRGS, and NOD-RG mice were irradiated with 670, 580, and 420 cGy, respectively. Each dose was set by irradiation tolerance experiments (see the Methods).

At 8 weeks after transplantation, human CD45$^+$ cells were not detectable in C57BL/6-RG mice (Figure 2A). Both BRGS and NOD-RG showed successful reconstitution and their average frequencies of human CD45$^+$ cells were 59.9% and 55.8%, respectively. Recent studies have shown that in the NSG strain,[15] female recipients better support the reconstitution of human hematopoiesis, although the underlying mechanism for this remains unclear.[38,39] As shown in Figure 2A, NOD-RG and BRGS female mice showed equally excellent human CD45$^+$ reconstitution at approximately 70% chimerism. NOD-RG male mice, however, showed significantly poor reconstitution (16.6% of human cell chimerism on average) compared with NOD-RG female mice. In contrast, the percentages of human cell chimerisms in BRGS male mice (approximately 45%) were only slightly lower than those in BRGS female mice and, as a result, BRGS male mice showed significantly better engraftment compared with NOD-RG male mice.

In the BM, the percentages of CD19$^+$ B cells, CD33$^+$ myeloid cells, and CD34$^+$CD38$^-$ cells that contain the majority of human HSCs were almost equal between the BRGS and the NOD-RG strains irrespective of sex (Figure 2B). Representative FACS plots at 8 weeks after injection are shown in Figure 3A. In the spleen, small numbers of CD3$^+$ T cells and CD3$^-$NKp46$^+$ NK cells, as well as CD41$^+$ megakaryocytes and CD235a$^+$ erythrocytes, were found in both BRGS and NOD-RG mice (Figure 3A) and there was no significant difference in the percentages of these cells between the 2 strains regardless of sex. The majority of human cells in the spleen were CD19$^+$ B cells (Figure 3B). Although BM human

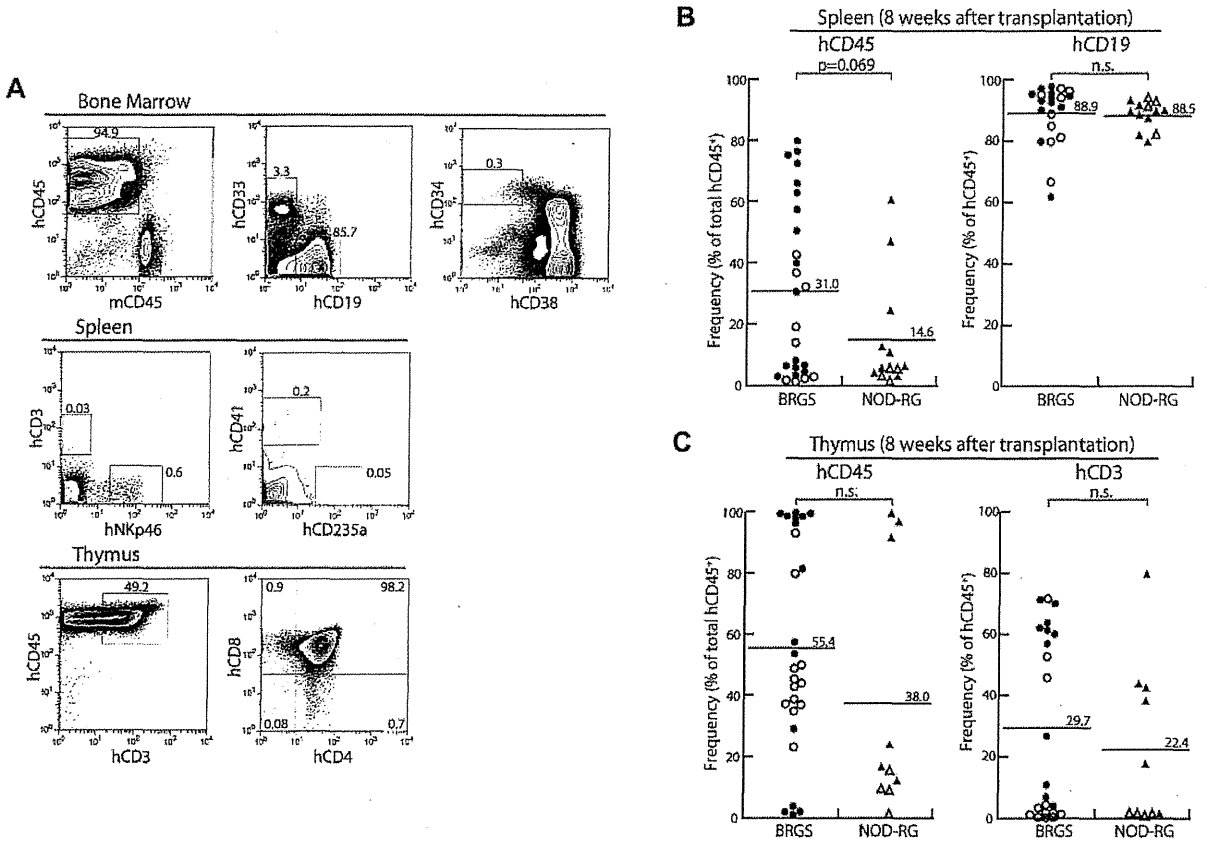

Figure 3. Multilineage human HSC reconstitution in BRGS mice. (A) Representative FACS plots at 8 weeks after transplantation in the BM, spleen, and thymus. (B) *Human hematopoietic reconstitution in the spleens of BRGS and NOD-RG recipients (●: BRGS female; ○: BRGS male; ▲: NOD-RG female; △: NOD-RG male).* There were no significant differences in the percentages of human CD45+ cells and human CD19+ B cells between these mice. (C) Human hematopoietic reconstitution in the thymi of BRGS and NOD-RG recipients. There were no significant differences in the percentages of human CD45+ cells and human CD3+ T cells between these mice. Symbols are as in panel B.

$CD19^+$ cells were mainly $CD10^+CD20^-$ immature B cells, the majority (approximately 90%) of human spleen $CD19^+$ cells were $CD10^-CD20^+$ mature B cells (data not shown). Thymic T cells were found in both the BRGS and NOD-RG strains, and the majority of human $CD3^+$ T cells in the thymus were $CD4^+CD8^+$ immature T cells (Figure 3A,C).

Figure 4 shows the analysis of reconstitution of human HSCs at 16 weeks after transplantation. In this analysis, we used only female BRGS and NOD-RG mice. In the BM, both BRGS and NOD-RG mice showed sustained human cell engraftment and the frequencies of human $CD45^+$ cells were 64.4% and 51.1% in average, respectively, which were comparable to their levels at 8 weeks after transplantation. The percentages of $CD33^+$ myeloid cells, $CD19^+$ B cells, and $CD34^+CD38^-$ HSCs were comparable to those at 8 weeks after transplantation (Figure 4A).

In the thymus, the percentage of $CD3^+$ T cells was increased up to approximately 80% and approximately 60% in the BRGS and NOD-RG strains, respectively. In addition to $CD4^+CD8^+$ thymic precursors, both $CD4^+$ and $CD8^+$ single-positive T cells were present and expressed surface TCR-αβ or TCR-γδ, suggesting that human T-cell maturation occurs in the BRGS thymus, as has been shown previously in the NOG, NSG, and NOD-RG mouse lines[14-16,20] (Figure 4B). The number of $CD20^+$ mature B cells in the spleen was increased and they expressed surface Ig light chain λ/κ, reflecting their normal maturation (Figure 4C).

The BRGS mouse maintains self-renewal of human HSCs in the long term

Figure 5A shows the changes in human cell chimerism in female BRGS mice in the long term. The frequency of human $CD45^+$ cells was maintained at a high level at least until 24 weeks after transplantation. B-cell frequencies gradually declined, but human myeloid, T, and NK cells progressively increased after engraftment (Figure 5B). The delayed reconstitution of these lineages of human cells has also been reported in studies using NSG mice.[40,41]

Figure 5C shows the results of the serial transplantation analysis. After confirmation of human cell engraftment at 8 weeks after the first transplantation, 1×10^6 human $CD45^+$ cells were purified from primary BRGS recipients. These cells were transplanted into irradiated secondary BRGS recipients by intrafemoral injection and tested for engraftment after another 8 weeks. Four of 6 secondary BRGS recipients showed multilineage engraftment of human $CD33^+$, $CD19^+$, and $CD3^+$ cells (Figure 5C). These data strongly suggest that BRGS mice can support long-term reconstitution and self-renewal of human HSCs.

The BRGS mouse is useful for experiments using CDC of antibodies in the xenotransplantation setting

One of the problems in NOD-based xenograft models is that the cytotoxic activities of antibodies are unable to be evaluated in vivo